

# MODELING THE EFFECTS OF DRUGS OF ABUSE ON HIV INFECTIONS WITH TWO VIRAL SPECIES

Peter M. Uhl<sup>1</sup> and Naveen K. Vaidya<sup>1,2</sup>

<sup>1</sup>Computational Science Research Center, San Diego State University

<sup>2</sup>Department of Mathematics and Statistics, San Diego State University

February 18, 2019

## Abstract

Injection drug use is one of the greatest risk factors associated with contracting human immunodeficiency virus (HIV), and drug abusers infected with HIV suffer from a higher viral load and rapid pathogenesis. Replication of HIV may result in a large number of mutant viruses that can escape recognition of the host's immune response. Experimental results have shown that the presence of morphine can decrease the viral mutation rate and cellular immune responses. In this study, we present a mathematical model to determine if the decrease in mutation and cellular immune response in the presence of morphine can account for the increased viral load. Two viral species are considered: a wild-type and a mutant. The morphine-altered mutation rate and cellular immune response is shown to allow the wild-type virus to out compete the mutant, resulting in a higher set point viral load. Calculation of the basic reproduction number for each species shows that the dominant species is determined by a threshold morphine concentration, with the mutant dominating below the threshold and the wild-type dominating above. Stability analysis is performed on the infection free and mutant only equilibria of the system and numerical simulations reflect the increased viral load associated with morphine use.

## 1 Introduction

Human immunodeficiency virus (HIV) is a significant health concern in the United States and around the world, with about 56,000 new infections per year in the United States [1]. HIV is a blood borne pathogen and one of the most common forms of transmission is by the sharing of needles used for injecting drugs of abuse, such as opiodes, between infected and non- infected persons. Drugs of abuse have been shown to have adverse effects on the progression of HIV infections, including a higher set point viral load and decreased amounts of CD4+ T cells [2]. Studies involving rhesus macaques and simian immunodeficiency virus

(SIV and HSIV) have shown that morphine causes a faster progression to AIDS and a higher pathogenesis in affected animals, many other studies of HIV have also demonstrated that a quicker progression to AIDS maybe associated with opiate use [3]. It is therefore important to investigate the mechanisms by which morphine affects the progression of HIV infections and viral burden.

Cytotoxic T-lymphocytes (CTLs) are an important component of the human immune system for combating viral infections, including HIV, by limiting viral reproduction and the infection of hosts' target cells. In the acute stage of the infection the host's immune system responds by creating a large amount of virus specific CTLs. The CTLs perform actions to inhibit viral growth, for example by destroying infected cells directly. After the infection has progressed and the immune response by CTLs has been reduced it is possible for mutant viruses to revert back to the original wild-type strain. Therefore the production of CTLs plays a significant role in the progression of an infection [4]. However, HIV possesses a high genetic variability which results in the production of escape mutants that can avoid detection by CTLs [5]. The high number of CTLs puts pressure on the virus to quickly mutate to a form that can evade the CTLs, this combined with the quick replication speed of HIV results in a large number of mutant viruses being produced [13, 14]. The production of mutant viruses can be a significant barrier to the treatment of HIV by antiviral drugs or to the development of an effective vaccine [5].

Experimental studies have shown that opiates can increase viral replication by increasing CCR5 expression in target cells [16] and studies on rhesus macaques have shown similar levels of viral growth in the early stages of infection between morphine dependent and control animals, but higher set point viral loads associated with morphine use [2]. Morphine has also been shown to affect the amount of escape mutants that evolve, but the exact effect remains unclear [17]. Mathematical models have been very useful in understanding the dynamics of infectious diseases [6, 7]. A problem on which there has been little study is to determine the effects of morphine on the viral dynamics of HIV when multiple viral species are present, and the objective of this paper is to present such a model. Thus, it is desirable to develop a mathematical model that will include components for the host's cellular immune response (CTLs), escape mutations, and morphine use.

## 2 Method

### 2.1 Model

The model can be written as the following system of differential equations:

$$\begin{aligned}
T_l' &= \lambda + q(M)T_h - r(M)T_l - \beta_l V_w T_l - (1 - F)\beta_l V_m T_l - \delta_T T_l \\
T_h' &= r(M)T_l - q(M)T_h - \beta_h V_w T_h - (1 - F)\beta_h V_m T_h - \delta_T T_h \\
V_w' &= pI_w - \delta_V V_w \\
V_m' &= pI_m - \delta_V V_m \\
I_w' &= (1 - \frac{\epsilon}{\mu + \eta M})(\beta_l V_w T_l + \beta_h V_w T_h) - bI_w C - \delta_I I_w \\
I_m' &= \frac{\epsilon}{\mu + \eta M}(\beta_l V_w T_l + \beta_h V_w T_h) + (1 - F)(\beta_l V_m T_l + \beta_h V_m T_h) - \frac{b}{1 + B}I_m C - \delta_I I_m \\
C' &= \omega + \frac{\alpha}{\gamma + \xi M}(I_w + I_m)C - \delta_C C
\end{aligned}$$

where  $T_l$  and  $T_h$  denote target cells,  $V_w$  and  $V_m$  are wild-type and mutant virus,  $I_w$  and  $I_m$  are cells infected by the wild-type and mutant virus, respectively, and  $C$  is CTLs. Two populations of target cells are included to model the increased susceptibility of some target cells caused by morphine use, so that  $T_h$  represents cells that are exhibiting increased co-receptor expression and are more likely to become infected than cells in the  $T_l$  population [22]. Two viral species are included to model the evolution of the virus, so that a portion of cells infected by the wild-type virus undergo mutation and go into the  $I_m$  population [20]. The host's cellular immune response is modeled by the population of CTLs, the production of which is stimulated by the presense of infected cells [20].

It is assumed that all newly created target cells belong to the  $T_l$  population and are produced at rate  $\lambda$ , and that target cells transision from  $T_l$  to  $T_h$  at rate  $r$  and from  $T_h$  to  $T_l$  at rate  $q$  [22]. Cells in the  $T_l$  population are infected by the wild-type virus at the per capita rate of  $\beta_l$  and by mutant virus at per capita rate  $(1 - F)\beta_l$ , where  $F$  is the fitness cost of the mutation. Similarly,  $T_h$  cells are infected at rates  $\beta_h$  and  $(1 - F)\beta_h$ . Both populations of target cells die at  $\delta_T$  [6, 21].

Both species of virus proliferate at rate  $p$  in proportion to the amount of target cells and are cleared at rate  $\delta_V$  [20]. Due to mutation, a fraction  $\epsilon$  of target cells infected by wild-type virus become mutant infected cells and the remainder,  $(1 - \epsilon)$  become wild-type infected cells [20]. Wild-type infected cells are cleared by CTLs at rate  $b$ . Due to responses by epitope-specific CTLs there is some recognition of the mutant by CTLs [20, 29], so the clearance rate of the mutant virus by CTLs is modeled by  $\frac{b}{1+B}$ , where  $1 + B$  is the escape ratio- a reduction in the ability of CTLs to kill mutant infected cells. Infected cells die at per capita rate  $\delta_I$ . CTLs are produced at constant rate  $\omega$ , die at rate  $\delta_C$ , and are also produced at rate  $\alpha$  in proportion to the total number of infected cells,  $I_w + I_m$  [20].

The effect of morphine on these dynamics will be modeled through three mechanisms: the increase in the  $T_h$  population, the decrease in mutation, and the decrease in CTL production. Morphine changes the rates of transition between target cell populations, giving  $q(M)$  and  $r(M)$ , by decreasing  $r(M)$  and decreasing  $q(M)$  resulting in more target cells in the  $T_h$  population [22]. This is modeled using an e-max model of the form

$$\begin{aligned} r(M) &= r_c + (r_m - r_c)\eta_r(M) \\ q(M) &= q_m + (q_c - q_m)\eta_q(M) \end{aligned}$$

where

$$\begin{aligned} \eta_r(M) &= \frac{M^n}{M_h^n + M^n} \\ \eta_q(M) &= 1 - \eta_r(M). \end{aligned}$$

The decrease in viral mutation brought on by morphine is modeled by introducing parameters  $\mu$  and  $\eta$  and reducing  $\epsilon$  in proportion to the concentration of morphine,  $M$ , so that the mutation rate in the presence of morphine is  $\frac{\epsilon}{\mu + \eta M}$ . Similarly, the decrease in CTL production can be modeled by introducing parameters  $\gamma$  and  $\xi$  so that the CTL production in response to infection is  $\frac{\alpha}{\gamma + \xi M}$  when morphine is present. Finally, the constant rate of CTL production is assumed to decrease exponentially with decay rate  $\psi$  when morphine is present, so that the new rate of CTL production is  $\omega e^{-\psi M}$ .

## 2.2 Parameter Estimates

Estimates for parameter values are taken from previously published studies. Following Vaidya et al. [22], we assume  $10^6$  target cells per  $ml$  of blood, about  $40980/ml$  belonging to the  $T_l$  population and the remaining  $10^6 - 40980/ml$  to the  $T_h$  population. Since there are initially no infected cells, we take  $I_w = I_m = 0$ . We estimate the initial viral load  $V_0$  based on experimental work. In [2], rhesus macaques were infected intravenously with 2-ml inoculum containing a cocktail of three SIV viruses. The cocktail contained  $10^5$  HIV RNA copies of each of the three viruses, and assuming a macaque contains approximately 1.5 liters of extracellular water we can estimate  $V_0 = \frac{3 \times 10^5}{1.5L} \approx 200$  viral RNA copies/ml [22], which we assume belongs entirely to the  $V_w$  population. Estimates for  $\lambda, \beta_l, \beta_h, r$ , and  $q$  were taken from Vaidya et al. [22], where they were obtained by fitting their model to experimental data. In particular, the observed  $\beta_l$  to be approximately two orders of magnitude lower than  $\beta_h$ . The fitness cost  $F$  will vary between 0 and 1.

Previous estimates give the average viral clearance rate as 23 cells per day and the average target cell life span as 100 days, so we take  $\delta_V = 23$  and  $\delta_T = 1/100 = 0.01$  [30, 31]. We assume only forward-mutation takes place, i.e., that mutant infected cells will not revert to wild-type infected cells, and take the mutation rate as  $\epsilon = 3 \times 10^{-5}$  obtained experimentally in [32]. The parameters  $\mu$  and  $\eta$  that account for the effect of morphine on  $\epsilon$  will vary. Following Konrad, we take the CTL death rate  $\delta_C \approx 10^{-1}$  and use the estimate for the CTL production rate  $\alpha = 6.7 \times 10^{-5}$  obtained by De Boer and Perelson [20, 34]. The parameters  $\gamma$  and  $\xi$  that account for the effect of morphine on  $\alpha$  will vary. Previous modeling work by Ganusov gives a range of the CTL killing rate,  $b$ , between 0.01 and 0.4 [27] and the escape ratio  $B$  will be varied.

We assume that the constant rate of CTL production,  $\omega$  is 50 cells per day in the absence of morphine and decays exponentially with respect to the morphine concentration, giving  $\hat{\omega}(M) = \omega e^{-\psi M}$  with decay rate  $\psi$ . Olkkola et al measured the kinetics and dynamics of morphine in children and observed initial concentrations of morphine between 28 and 325  $\mu\text{l}$  per kilogram of body weight, therefore we will take  $M$  between 0 and 300 [24].

The estimated parameters and their descriptions are summarized in Table 1:

Table 1: Parameter Values

| Parameter  | Value   | Description                              | Reference        |
|------------|---|--|------------------|
| $\lambda$  | $3690 \text{ ml}^{-1} \text{ day}^{-1}$                     | Production rate of $T_l$ cells           | Vaidya et al.    |
| $r_c$      | $0.16 \text{ day}^{-1}$                                     | Minimum value of $r$                     | Vaidya et al.    |
| $r_m$      | $0.52 \text{ day}^{-1}$                                     | Maximum value of $r$                     | Vaidya et al.    |
| $q_c$      | $1.23 \times 10^{-6} \text{ day}^{-1}$                      | Minimum value of $q$                     | Vaidya et al.    |
| $q_m$      | $0.25 \text{ day}^{-1}$                                     | Maximum value of $q$                     | Vaidya et al.    |
| $M_h$      | $2.8534 \times 10^{-3}$                                     |  | ???              |
| $n$        | 7.8731  |  | ???              |
| $\beta_l$  | $10^{-9} \text{ cells}^{-1} \text{ ml day}^{-1}$            | Wild- type infection rate of $T_l$ cells | Vaidya et al.    |
| $\beta_h$  | $10^{-7} \text{ cells}^{-1} \text{ ml day}^{-1}$            | Wild -type infection rate of $T_h$ cells | Vaidya et al.    |
| $F$        | $0 - 1$   | Fitness cost of mutation                 | Varied           |
| $p$        | $4000 \text{ day}^{-1}$                                     | Production rate of virus                 | Vaidya et al.    |
| $b$        | $0.01 - 0.4 \text{ cells}^{-1} \text{ ml day}^{-1}$         | CTL killing rate of wild- type           | Ganusov et al.   |
| $B$        | $1 - 100$   | Escape ratio                             | Varied           |
| $\alpha$   | $6.7 \times 10^{-6} \text{ cells}^{-1} \text{ ml day}^{-1}$ | CTL proliferation rate                   | De Boer et al.   |
| $\gamma$   | $0.4 - 1$   | Morphine parameter affecting $\alpha$    | Varied           |
| $\xi$      | $0.4 - 1$   | Morphine parameter affecting $\alpha$    | Varied           |
| $\omega$   | 50  | CTL production rate                      | Varied           |
| $\psi$     | 0.05  | CTL prduction decay rate                 | Varied           |
| $\epsilon$ | $3 \times 10^{-5}$  | Mutation rate                            | Mansky et al.    |
| $\mu$      | $0.1667 - 1$  | Morphine parameter affecting $\epsilon$  | Varied           |
| $\eta$     | $0.1667 - 1$  | Morphine parameter affecting $\epsilon$  | Varied           |
| $\delta_T$ | $0.01 \text{ day}^{-1}$                                     | Target cell death rate                   | Stafford et al.  |
| $\delta_V$ | $23 \text{ day}^{-1}$                                       | Virus clearance rate                     | Ramratnam et al. |
| $\delta_I$ | $0.3 \text{ day}^{-1}$                                      | Infected cell death rate                 | Vaidya et al.    |
| $\delta_C$ | $0.63 \text{ day}^{-1}$                                     | CTL death rate                           | Konrad et al.    |
| $M$        | $0 - 300 \text{ ml/kg}$                                     | Concentration of morphine                | Oikkola et al.   |

### 3 Results

#### 3.1 Basic Reproduction Number

The basic reproduction number, denoted  $R_0$ , is an important quantity in the study of viral dynamics and is defined as the average number of secondary infected cells resulting from a single initial infected cell when target cells are not limited [23]. The stability of the infection free equilibrium (IFE) can be described by the basic reproduction number, with the IFE being locally asymptotically stable if  $R_0 < 1$  and unstable if  $R_0 > 1$  [23]. Since our model contains two viral species the basic reproduction number is obtained, as we show below, as a combination of the reproduction numbers  $R_0^w$  and  $R_0^m$ , corresponding to the wild-type and mutant viruses, respectively.

For our model, the IFE is  $(T_l^*, T_h^*, 0, 0, 0, 0, C^*)$  where

$$\begin{aligned} T_l^* &= \frac{\lambda(q(M) + \delta_T)}{\delta_T(q(M) + r(M) + \delta_T)}, \\ T_h^* &= \frac{\lambda r(M)}{\delta_T(q(M) + r(M) + \delta_T)}, \\ C^* &= \frac{\hat{\omega}}{\delta_C}. \end{aligned}$$

Here, we use the next generation method [35] to obtain an expression for the basic reproduction number of the model. The next-generation matrix is obtained from the infected subsystem of the model, i.e., the equations of the system that contain viruses and infected cells [35]. For our model, the infected subsystem is given by

$$\begin{aligned} V_w' &= pI_w - \delta_V V_w \\ V_m' &= pI_m - \delta_V V_m \\ I_w' &= (1 - \hat{\epsilon})(\beta_l V_w T_l + \beta_h V_w T_h) - bI_w C - \delta_I I_w \\ I_m' &= \hat{\epsilon}(\beta_l V_w T_l + \beta_h V_w T_h) + (\hat{\beta}_l V_m T_l + \hat{\beta}_h V_m T_h) - \frac{b}{1+B} I_m C - \delta_I I_m \end{aligned}$$

The next step is to linearize the infected subsystem about the IFE and decompose it into  $\mathcal{F} - \mathcal{V}$ , where  $\mathcal{F}$  is the infection part of the system, which describes newly infected components, and  $\mathcal{V}$  is the transition part, which describes transitions of cells and viruses in and out of compartments.  $\mathcal{F}$  and  $\mathcal{V}$  for our model are given by

$$\mathcal{F} = \begin{bmatrix} 0 & 0 & 0 & 0 \\ 0 & 0 & 0 & 0 \\ (1 - \hat{\epsilon})(\beta_l T_l^* + \beta_h T_h^*) & 0 & 0 & 0 \\ \hat{\epsilon}(\beta_l T_l^* + \beta_h T_h^*) & \hat{\beta}_l T_l^* + \hat{\beta}_h T_h^* & 0 & 0 \end{bmatrix}$$

and

$$\mathcal{V} = \begin{bmatrix} \delta_V & 0 & -p & 0 \\ 0 & \delta_V & 0 & -p \\ 0 & 0 & \delta_I + bC^* & 0 \\ 0 & 0 & 0 & \delta_I + \frac{b}{1+B}C^* \end{bmatrix}.$$

The next generation matrix is  $\mathcal{FV}^{-1}$  and its spectral radius  $\sigma(\mathcal{FV}^{-1})$  is the basic reproduction number of the system. The basic reproduction number of our model is thus obtained as  $R_0 = \sigma(\mathcal{FV}^{-1}) = \max\{R_0^w, R_0^m\}$ , where

$$R_0^w = -\frac{p(T_h^* \beta_h \hat{\epsilon} + T_l^* \beta_l \hat{\epsilon} - T_h^* \beta_h - T_l^* \beta_l)}{(\delta_I + bC^*)\delta_V}$$

$$R_0^m = -\frac{p(BFT_h^* \beta_h + BFT_l^* \beta_l - BT_h^* \beta_h - BT_l^* \beta_l + FT_h^* \beta_h + FT_l^* \beta_l - T_h^* \beta_h - T_l^* \beta_l)}{(B\delta_I + C^*b + \delta_I)\delta_V}.$$

Here  $R_0^w$  and  $R_0^m$  correspond to the basic reproduction number of the wild-type and mutant virus, respectively. In order to observe the effect of morphine on  $R_0$ , and therefore on the viral load,  $R_0^w$  and  $R_0^m$  are calculated for various concentrations of morphine, noting that if  $R_0^w > R_0^m$  the wild-type virus will be the dominate viral species while if  $R_0^w < R_0^m$  the mutant will dominate. Using the Parameter values in Table 1 and letting  $M$  vary from 0 to 300 gives the results shown Figure 1.

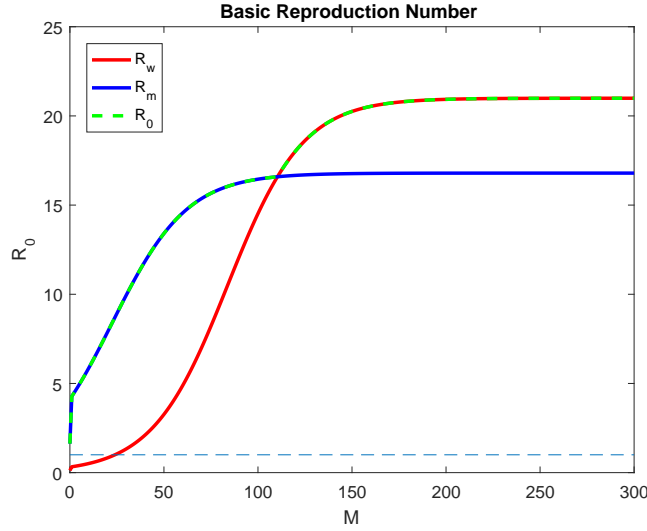


Figure 1: Computed values of  $R_w$  and  $R_m$  for increasing  $M$ . A population switch occurs at approximately  $M = 100$ .

Setting  $M = 0$  results in  $R_0 = R_m = 1.63$ , indicating that the mutant virus is dominant when there is no morphine and that the IFE is unstable. A population switch occurs at approximately  $M = 100$  and the wild-type becomes dominant for any higher morphine concentrations. Note that  $M = 300$  results in  $R_0 = R_w \approx 21$ . In the next section, simulations of the steady state viral load will show that the dominance of the mutant virus contributes to the higher viral load when morphine is present.

We now perform a sensitivity analysis to identify the parameters that have the greatest effect on the basic reproduction number [33]. For a parameter  $x$ , the forward sensitivity index is given by [36, 37]

$$S_x = \frac{x}{R_0} \frac{\partial R_0}{\partial x}.$$

Using the parameter values in Table 1, the sensitivity indices for  $R_0^w$  and  $R_0^m$  are given in the bar graphs below.

## 3.2 Stability Analysis

### 3.2.1 Mutant Only Equilibrium

The mutant only equilibrium is the equilibrium in which there is no wild-type virus present  $(T_l^*, T_h^*, 0, V_m^*, 0, I_m^*, C^*)$ , where



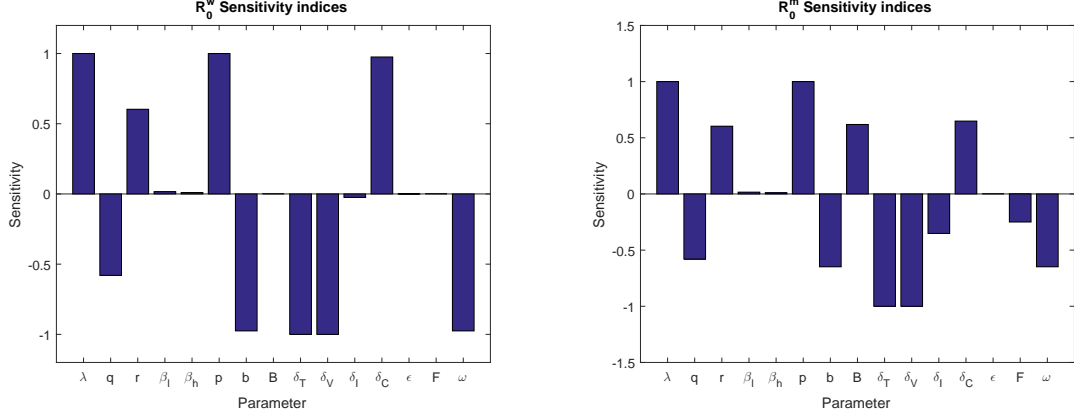


Figure 2: Sensitivity indices for  $R_0^w$  and  $R_0^m$

$$\begin{aligned}
T_h^* &= \frac{r(M)\lambda}{(q(M) + \hat{\beta}_h V_m^* + \delta_T)(r(M) + \hat{\beta}_l V_m^* + \delta_T) - r(M)q(M)} \\
T_l^* &= \frac{\lambda(q(M) + \hat{\beta}_h V_m^* + \delta_T)}{(q(M) + \hat{\beta}_h V_m^* + \delta_T)(r(M) + \hat{\beta}_l V_m^* + \delta_T) - r(M)q(M)} \\
I_m^* &= \frac{\delta_V V_m^*}{p} \\
C^* &= \frac{\omega}{\delta_C - \hat{\alpha} \frac{\delta_V V_m^*}{p}}
\end{aligned}$$

and  $V_m^*$  is the solution of

$$0 = V_m^* \cdot g(V_m^*)$$

where

$$g(V_m^*) = \frac{\hat{\beta}_l \lambda \left( V_m^* \hat{\beta}_h + q(M) + \delta_T \right) + \hat{\beta}_h r \lambda}{\left( V_m^* \hat{\beta}_h + q(M) + \delta_T \right) \left( V_m^* \hat{\beta}_l + r(M) + \delta_T \right) - r(M)q(M)} - \frac{b \delta_V \omega}{(1+B)p \left( \delta_C - \frac{\hat{\alpha} \delta_V V_m^*}{p} \right)} - \frac{\delta_I \delta_V}{p}.$$

Clearly,  $V_m^* = 0$  satisfies this equation, but this results in the IFE. The zeros of  $g(V_m^*)$  can be found numerically and are plotted below for different values of  $M$ .

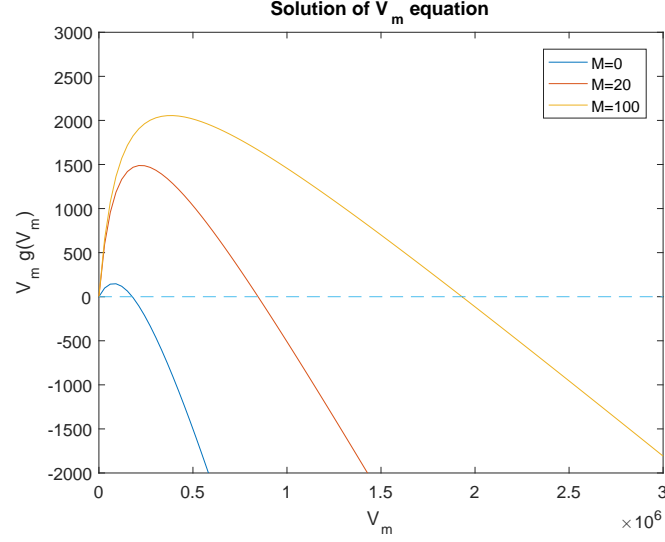


Figure 3: Solutions of  $V_m^*$  equation. The zero-intercept of each curve is the MOE value of  $V_m$  for the particular value of  $M$ .

To determine the stability of the MOE, we calculate the Jacobian matrix and evaluate it at the MOE. The Jacobian matrix is

$$J = \begin{bmatrix} J_{11} & J_{12} & J_{13} & J_{14} & 0 & 0 & 0 \\ J_{21} & J_{22} & J_{23} & J_{24} & 0 & 0 & 0 \\ 0 & 0 & J_{33} & 0 & J_{35} & 0 & 0 \\ 0 & 0 & 0 & J_{44} & 0 & J_{46} & 0 \\ J_{51} & J_{52} & J_{53} & 0 & J_{55} & 0 & J_{57} \\ J_{61} & J_{62} & J_{63} & J_{64} & 0 & J_{66} & J_{67} \\ 0 & 0 & 0 & 0 & J_{75} & J_{76} & J_{77} \end{bmatrix}$$

where

$$\begin{aligned}
J_{11} &= -r - \beta_l V_w - \hat{\beta}_l V_m - \delta_T & J_{52} &= (1 - \hat{\epsilon})\beta_h V_w \\
J_{12} &= q & J_{53} &= (1 - \hat{\epsilon})(\beta_l T_l + \beta_h T_h) \\
J_{13} &= -\beta_l T_l & J_{55} &= -bC - \delta_I \\
J_{14} &= -\hat{\beta}_l T_l & J_{57} &= -bI_w \\
J_{21} &= r & J_{61} &= \hat{\epsilon}\beta_l V_w + \hat{\beta}_l V_m \\
J_{22} &= -q - \beta_h V_w - \hat{\beta}_h V_m - \delta_T & J_{62} &= \hat{\epsilon}\beta_h V_w + \hat{\beta}_h V_m \\
J_{23} &= -\beta_h T_h & J_{63} &= \hat{\epsilon}(\beta_l T_l + \beta_h T_h) \\
J_{24} &= -\hat{\beta}_h T_h & J_{64} &= \hat{\beta}_l T_l + \hat{\beta}_h T_h \\
J_{33} &= -\delta_V & J_{66} &= -\frac{b}{1+B}C - \delta_I \\
J_{35} &= p & J_{67} &= -\frac{b}{1+B}I_m \\
J_{44} &= -\delta_V & J_{75} &= \hat{\alpha}C \\
J_{46} &= p & J_{76} &= \hat{\alpha}C \\
J_{51} &= (1 - \hat{\epsilon})\beta_l V_w & J_{77} &= \hat{\alpha}(I_w + I_m) - C.
\end{aligned}$$

Note that the MOE is locally asymptotically stable if the real parts of each eigenvalue of  $J$  is negative and unstable otherwise [25, 28]. We now examine how the amount of morphine affects the stability of the MOE. We compute the maximum of the real parts of all eigenvalues of  $J$  as a function of  $M$ , shown in Figure 4. Note that the real parts plotted in Figure 4 do not necessarily belong to the same eigenvalue. The MOE becomes unstable at  $M \approx 110$ , later we show that the wild-type virus dominates when  $M$  exceeds this value.

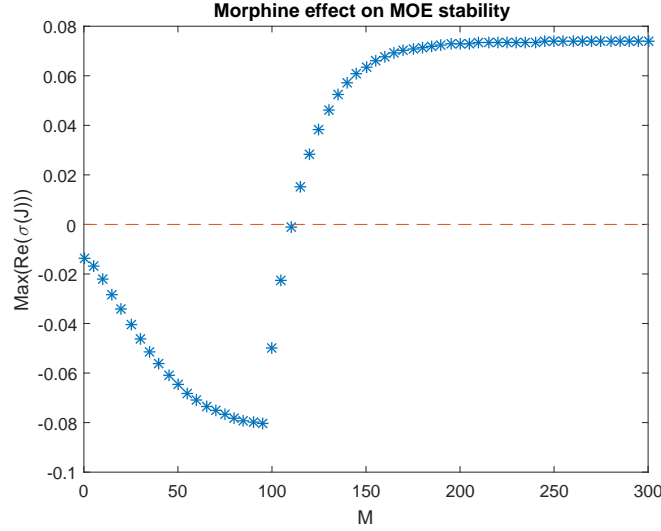


Figure 4: Effect of  $M$  on the stability of the MOE. The MOE becomes unstable at approximately  $M = 110 \text{ ml/kg}$ .

The fitness cost  $F$  and escape ratio  $B$  also affect the stability of the MOE. The contour plot in Figure 5 shows the maximum real part of the eigenvalues of  $J$  evaluated at the MOE as a function of both  $F$  and  $M$ . Contours with a value less than 0 correspond to regions where the MOE is stable, and the figure shows that a low fitness cost can allow the mutant to dominate for higher concentrations of morphine.

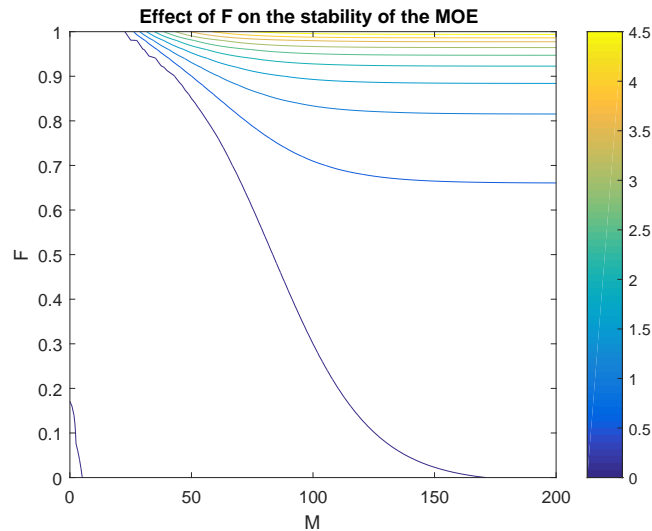


Figure 5: Effect of  $F$  on the stability of the MOE

The contour plot in Figure 6 shows the maximum real part of the eigenvalues of  $J$  evaluated at the MOE as a function of  $B$  and  $M$ . Contours with a value less than 0 correspond to regions where the MOE is stable.

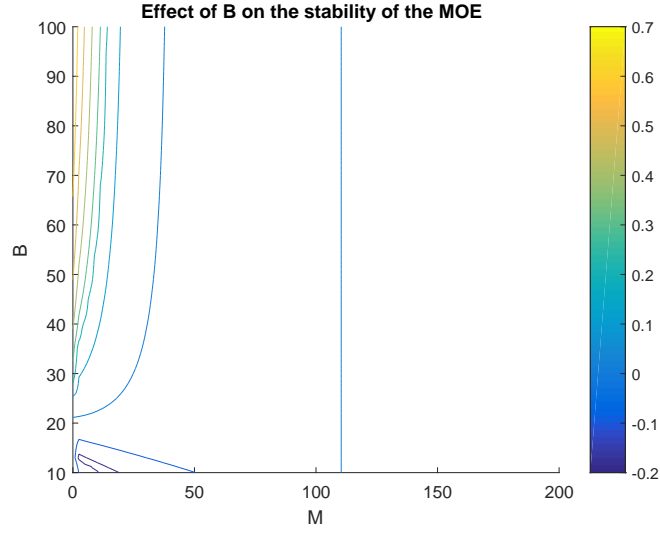


Figure 6: Effect of  $B$  on the stability of the MOE

### 3.2.2 Wild-type Only Equilibrium

A wild-type only equilibrium is a nonnegative solution of the form  $(T_l^*, T_h^*, V_w^*, 0, I_w^*, 0, C^*)$  to the system of equations

$$\begin{aligned}
 0 &= \lambda + qT_h - rT_l - \beta_l V_w T_l - \delta_T T_l \\
 0 &= rT_l - qT_h - \beta_h V_w T_h - \delta_T T_h \\
 0 &= pI_w - \delta_V V_w \\
 0 &= (1 - \hat{\epsilon})(\beta_l V_w T_l + \beta_h V_w T_h) - bI_w C - \delta_I I_w \\
 0 &= \hat{\epsilon}(\beta_l V_w T_l + \beta_h V_w T_h) \\
 0 &= \omega + \hat{\alpha} I_w C - \delta_C C.
 \end{aligned}$$

Solving the second equation for  $T_h^*$  gives:

$$T_h^* = \frac{r}{q + \beta_h V_w^* + \delta_T} T_l^*$$

and the fifth equation is equivalent to (since  $\epsilon \neq 0$ )

$$0 = \beta_l V_w T_l + \beta_h V_w T_h.$$

If  $V_w^* = 0$  this system is exactly the IFE, so cancelling  $V_w^*$  and substituting  $T_h^*$  gives:

$$0 = T_l^* (\beta_l + \beta_h (\frac{r}{q + \beta_h V_w^* + \delta_T}))$$

so either  $T_l^* = 0$  or  $\beta_l + \beta_h (\frac{r}{q + \beta_h V_w^* + \delta_T}) = 0$ . Substituting  $T_l^* = 0$  into the first equation results in the negative solution  $T_h^* = -\frac{\lambda}{q}$ . Letting  $\beta_l + \beta_h (\frac{r}{q + \beta_h V_w^* + \delta_T}) = 0$  is equivalent to

$$V_w^* = -\frac{1}{\beta_h} (\frac{\beta_h r}{\beta_l} + q + \delta_T)$$

which is also a negative solution, and there is no nonnegative wild-type only equilibrium.

### 3.3 Long-term Viral Dynamics

Using the initial values and parameters given in Section 2.2 along with  $F = 0.2$ ,  $B = 20.5$ ,  $\psi = 0.05$  and  $\mu = \eta = \gamma = \xi = 1$  the model is solved using the ode15s function in MATLAB over a period of 100 days.

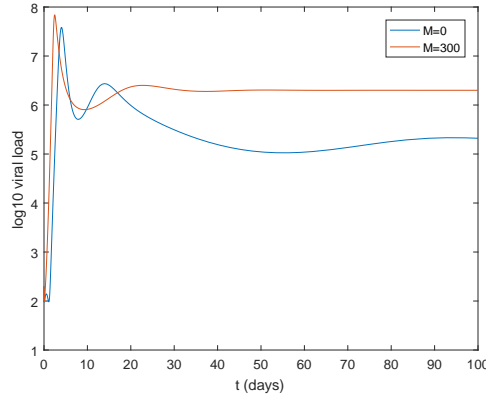
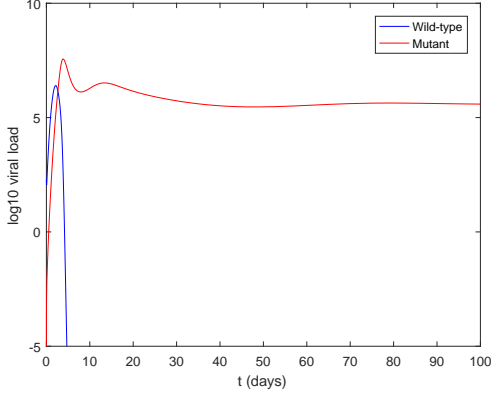


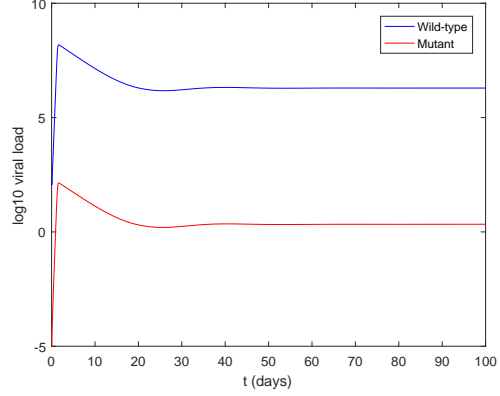
Figure 7: Total viral load with base parameter values. The model reflects the higher viral load caused by morphine.

Both cases show a rapid initial increase in viral load, but the presence of morphine causes a higher peak viral load and steady state than the control simulation. Analysis of the basic reproduction number showed that a population switch occurs at approximately  $M = 100\text{ml/kg}$ , so it is of interest to observe how the individual viral populations behave for values of  $M$  above and below the threshold value. With  $M = 0$ , the wild-type viral load

quickly declines to zero and the total viral load is entirely mutant virus. With  $M = 150$ , the wild-type virus is the dominant species but due to mutation there is a small amount of mutant virus being continuously produced. These simulations are consistent with the analysis of the basic reproduction number and its dependence on  $M$ .



(a) Individual viral populations,  $M = 0$



(b) Individual viral populations,  $M = 150$

## 4 Discussion

We present a mathematical model to describe the within-host viral dynamics of an HIV infection which considers escape mutants, the use of morphine, and different populations of target cells based on susceptibility to infection. The model is primarily based on earlier models from [22, 20] and simulates the increase in viral load that results from the use of morphine by introducing terms that lower the mutation rate of the virus and host's cellular immune response. Values of parameters in the model were taken both from earlier studies that provided estimates and from experimental data.

The basic reproduction number of each viral species is calculated by way of the next-generation matrix method. The basic reproduction number was taken as a function of the concentration of morphine present and it was observed that a population switch occurs for a sufficiently high morphine concentration. At higher concentrations of morphine the wild-type virus dominates the mutant, but the reduced cellular immune response still results in a higher set point viral load. The infection free equilibrium is unstable regardless of whether or not morphine is present. The mutant only equilibrium is also stable for a sufficiently low morphine concentration and fitness cost of the virus, but becomes unstable as these parameters increase.

Short- and long-term viral dynamics are simulated by solving the model numerically. If there is sufficient morphine for the wild-type virus to dominate a small amount of the mutant will persist due to mutation. If the mutant is the dominant species then it will effectively

make up the entirety of the viral load. Varying the morphine concentration causes changes in the set point viral load for low concentrations, but the viral load stabilizes once the morphine concentration exceeds approximately 100ml/kg.

One limitation of the model is the assumption that the morphine concentration  $M$  is constant with respect to time. This assumption is made for simplicity in calculations and for providing an easy way to determine the morphine concentration necessary for the population switch to occur. Future work will focus on developing a method to incorporate a time-dependent morphine concentration and determining how this would affect the dynamics. It will also be of interest to investigate the sensitivity of the parameters introduced to model morphine effects, namely  $\mu, \eta, \gamma$  and  $\xi$ , establish for them, and determining their effect on the stability of the equilibria of the model. Additionally, since it is possible for both the infection free and mutant only equilibria to be unstable it will be important to investigate any scenarios in which the wild-type and mutant coexist.

## References

- [1] *Morbidity and mortality weekly report*. vol. 59 (2010) pp. 1550-1555.
- [2] R. Kumar, C. Torres, Y. Yamamura, I. Rodriguez, M. Martinez, S. Staprans, R. M. Donahoe, E. Kraiselburd, E. B. Stephens, and A. Kumar, *Modulation by morphine of viral set point in rhesus macaques infected with simian immunodeficiency virus and simian-human immunodeficiency virus*, J. Virol. vol. 78 (2004) pp. 11425-11428.
- [3] K. F. Hauser, Y. K. Hahn, V. V. Adjan, S. Zou, S. K. Buch, A. Nath, A. J. Bruce-Kelle, and P. E. Knapp, *HIV-1 tat and morphine have interactive effects on oligodendrocyte survival and morphology*, Glia vol. 57 (2009) pp. 194-206. doi:10.1002/glia.20746.
- [4] T. C. Greenough, D. B. Brettler, M. Somasundaran, D. L. Panicali and J. L. Sullivan, *Human immunodeficiency virus type 1- specific cytotoxic T lymphocytes (CTL), virus load, and CD4 T cell loss: evidence supporting a protective role for CTL in vivo*, J. Infect. Dis. vol. 176 (1997) pp. 118-125.
- [5] C. L. Boutwell, M. M. Rolland, J. T. Herbeck, J. I. Mullins, and T. M. Allen, *Viral evolutions and escape during acute HIV-1 infection*, J. Infect. Dis. vol. 202 (2010) pp. S309-S314.
- [6] A. S. Perelson and R. M. Ribeiro, *Modeling the within-host dynamics of HIV infection*, BMC Biol. (2013) <http://www.biomedcentral.com/1741-7007/11/96>
- [7] M. C. Chubb and K. H. Jacobsen, *Mathematical modeling and the epidemiological research process*, Eur. J. Epidemiol. vol. 25 (2010) pp. 13-19.
- [8] S. G. Kitchen, J. K. Whitmire, N. R. Jones, Z. Galic, C. M. R. Kitchen, R. Ahmed, J. A. Zack, and F. V. Chisari, *The CD4 molecule on CD8+ T lymphocytes directly enhances the immune response to viral and cellular antigens*, Proc. Natl. Acad. Sci. U.S.A. vol. 102 (2005) pp. 3794-3799.



- [9] N. Kileen, C. B. Davis, K. Chu, M. E. C. Crooks, S. Sawada, J. D. Scarborough, K. A. Boyd, S. G. Stuart, H. Xu, and D. R. Littman, *CD4 function in thymocyte differentiation and T cell activation*, Philos. Trans. R. Soc. Lond., B, Biol. Sci. vol. 342 (1993) pp. 25-34.
- [10] D. C. Chan and P. S. Kim, *HIV entry and its inhibition*, Cell. vol. 93 (1998) pp. 681-684.
- [11] A. S. Fauci, *Pathogenesis of HIV disease: Opportunities for new prevention interventions*, Clin. Infect. Dis. vol. 45 (2007) pp. S206-S212.
- [12] A. J. McMichael and S. L. Rowland-Jones, *Cellular immune responses to HIV*, Nature vol. 410 (2001) pp. 980-987.
- [13] L. Deng, M. Perteau, A. Rongvaux, L. Want, C. M. Durand, G. Ghiaur, J. Lai, H. L. McHugh, H. Hao, J. B. Margolick, C. Gurer, A. J. Murphy, D. M. Valenzuela, G. D. Yancopoulos, S. G. Deeks, T. Stowig, P. Kumar, J. D. Siliciano, S. L. Salzberg, R. A. Flavell, L. Shan, and R. F. Siliciano, *Broad CTL response is required to clear latent HIV-1 due to dominance of escape mutations*, Nature vol. 517 (2015) pp. 381-385.
- [14] R. M. Ribeiro, L. L. Chavez, D. Li, S. G. Self, and A. S. Perelson, *Estimation of the initial viral growth rate and basic reproductive number during acute HIV-1 infection*, J. Virol. vol. 84 (2010) pp. 6096-6102.
- [15] V. V. Ganusov, R. A. Neher, and A. S. Perelson, *Mathematical modeling of escape of HIV from cytotoxic T lymphocyte responses*, J. Stat. Mech. P01010-.foi:10.1088/1742-5468/2013/01/P01010.
- [16] Y. Li, X. Wang, S. Tian, C. Guo, S. D. Douglas, and W. Ho, *Methadone enhances human immunodeficiency virus infection of human immune cells*, J. Infect. Dis. vol. 185 (2002) pp. 118-122.
- [17] R. Noel, Z. Marrero-Otero, R. Kumar, G. S. Chompre-Gonzalez, A. S. Verma, and A. Kumar, *Correlation between SIV tat evolution and AIDS progression in cerebrospinal fluid of morphine-dependent and control macaques infected with SIV and SHIV*, Virology vol. 349 (2006) pp. 440-452.
- [18] R. Noel and A. Kumar, *SIV vpr evolution is inversely related to disease progression in a morphine-dependent rhesus macaque model of AIDS*, Virology vol. 359 (2007) pp. 397-404.
- [19] V. Rivera-Amill, P. S. Silverstein, R. Noel, S. Kumar, and A. Kumar, *Morphine and rapid disease progression in nonhuman primate model of AIDS: Inverse correlation between disease progression and virus evolution*, J. Neuroimmune Pharmacol vol. 5 (2014) pp. 122-132. <http://doi.org/10.1007/s11481-009-9184-0>
- [20] B. P. Konrad, N. K. Vaiyda, and R. J. Smith?, *Modeling mutation to a cytotoxic T-lymphocyte HIV vaccine*, Math. Popul. Stud. vol. 18 (2011) pp. 122-149.

- [21] E. S. Schwartz, K. R. H. Biggs, C. Bailes, K. A. Ferolito, and N. K. Vaidya, *HIV dynamics with immune responses: Perspectives from mathematical modeling*, Curr. Clin. Microbiol. Rep. vol. 3 (2016) pp. 216-224.
- [22] N. K. Vaidya, R. M. Ribeiro, A. S. Perelson, and A. Kumar, *Modeling the effects of morphine on simian immunodeficiency virus dynamics*, PloS Comput. Biol. (2016) <https://doi.org/10.1371/journal.pcbi.1005127>
- [23] C. Castillo-Chavez, Z. Feng, and W. Huang, *On the computation of  $R_0$  and its role on global stability*, Mathematical Approaches for Emerging and Reemerging Infections Diseases: An Introduction, Springer-Verlag, New York, 2002, pp. 229-250.
- [24] K. T. Olkkola, E. Maunuksela, R. Korpela, and P. H. Rosenberg, *Kinetics and dynamics of postoperative intravenous morphine in children*, Clin. Pharmacol. Ther. vol. 44 (1988) pp. 128-136.
- [25] L. Perko, *Differential equations and dynamical systems*, 2nd ed., Springer-Verlag, New York, 1991.
- [26] D. W. Jordan and P. Smith, *Nonlinear ordinary differential equations: An introduction to dynamical systems*, 3rd ed. Oxford University Press, New York, 1999.
- [27] V. V. Ganusov and R. J. De Boer, *Estimating costs and benefits of CTL escape mutations in SIV/HIV infection*, PloS Comput. Biol. (2006) <https://doi.org/10.1371/journal.pcbi.0020024>
- [28] R. J. Smith and L. M. Wahl, *Drug resistance in an immunological model of HIV-1 infection with impulsive drug effects*, Bull. Math. Biol. vol. 67 (2005) pp. 783-813.
- [29] D. H. Barouch, J. Kunstman, J. Glowczwskie, K. J. Kunstman, M. A. Egan, F. W. Peyerl, S. Santra, M. J. Kuroda, J. E. Schmitz, K. Beaudry, G. R. Krivulka, M. A. Lifton, D. A. Gorgon, S. M. Wolinsky, and N. L. Letvin, *Viral escape from dominant simian immunodeficiency virus epitope-specific cytotoxic T lymphocytes in DNA-vaccinated rhesus monkeys*, J. Virol. vol. 77 (2003) pp. 7367-7375.
- [30] B. Ramratnam, S. Bonhoeffer, J. Binley, A. Hurley, L. Zhang, J. E. Mittler, M. Markowitz, J. P. Moore, A. S. Perelson, and D. D. Ho, *Rapid production and clearance of HIV-1 and hepatitis C virus assessed by large volume plasma apheresis*, Lancet. vol. 354 (1999) pp. 1782.
- [31] M. A. Stafford, L. Corey, Y. Cao, E. S. Daar, D. D. Ho, and A. S. Perelson, *Modeling plasma virus concentration during primary HIV infection*, J. Theor. Biol. vol. 203 (2000) pp. 285-301.
- [32] L. M. Mansky and H. M. Temin, *Lower in vivo mutation rate of human immunodeficiency virus type 1 than that predicted from the fidelity of purified reverse transcriptase*, J. Virol. vol. 69 (1995) pp. 5087-5094.

- [33] S. Marino, I. B. Hogue, C. J. Ray, and D. E. Kirschner, *A methodology for performing global uncertainty and sensitivity analysis in systems biology*, J. Theor. Biol. vol. 254 (2008) pp. 178-196.
- [34] R. J. De Boer and A. S. Perelson, *Target cell limited and immune control models of HIV infection: A comparison*, J. Theor. Biol. vol. 190 (1998) pp. 201-214.
- [35] O. Diekmann, J. A. P. Heesterbeek, and M. G. Roberts, *The construction of next-generation matrices for compartmental epidemic models*, J. R. Soc. Interface (2009) <http://rsif.royalsocietypublishing.org/content/7/47/873>
- [36] S. D. Perera, S. S. N. Perera, and S. Jayasinghe, *Modeling and sensitivity of dengue viral dynamics*, Int. J. Curr. Res. vol. 8 (2006) pp. 34899-34906.
- [37] H. S. Rodrigues, M. T. T. Monteiro, and D. F. M. Torres, *Sensitivity analysis in a dengue epidemiological model*, Conference Papers in Mathematics vol. 2013 (2013).